Physica B 481 (2016) 86–90

Contents lists available at ScienceDirect

Physica B

journal homepage: www.elsevier.com/locate/physb

Competing magnetic anisotropies in obliquely deposited thin permalloy film

B.A. Belyaev [a,b,c], A.V. Izotov [a,b], P.N. Solovev [a,*]

[a] *Siberian Federal University, 79, pr. Svobodnyi, Krasnoyarsk 660041, Russia*
[b] *Kirensky Institute of Physics, Siberian Branch of the Russian Academy of Sciences, 50/38, Akademgorodok, Krasnoyarsk 660036, Russia*
[c] *Reshetnev Siberian State Aerospace University, 31, pr. Imeni Gazety "Krasnoyarskii Rabochii", Krasnoyarsk 660014, Russia*

ARTICLE INFO

Article history:
Received 10 September 2015
Received in revised form
26 October 2015
Accepted 28 October 2015
Available online 30 October 2015

Keywords:
Thin film
Magnetic anisotropy
Oblique deposition
Ferromagnetic resonance
Micromagnetic simulation

ABSTRACT

Distribution of the magnetic anisotropy in thin film prepared by thermal vacuum oblique deposition of permalloy with small off-normal angle of incident in the presence of an external magnetic field has been studied by ferromagnetic resonance technique. On local area of the sample, a mutual compensation of near orthogonal in-plane uniaxial magnetic anisotropies induced by oblique deposition and by applied magnetic field has been found. Moreover, in addition to the uniaxial (twofold) magnetic anisotropy, fourfold and sixfold magnetic anisotropies have been observed in the sample. To explain the obtained high-order anisotropies, we assumed that the sample has exchange coupled adjacent regions or phases with different parameters of magnetic anisotropy. The results of the micromagnetic analysis of a two-layer model of the sample confirm the hypothesis.

1. Introduction

Magnetic anisotropy is the fundamental property of thin films that has a strong impact on their static and dynamic magnetic behavior [1,2]. Generally, the intrinsic magnetic anisotropy of a thin polycrystalline ferromagnetic film is a sum of effective anisotropies originating from various mechanisms such as elastic stress, microstructure inhomogeneity, atomic pair ordering, and others [3]. Understanding of the role of each mechanism in the formation of the resulting anisotropy is crucial for producing samples with controllable magnetic properties designed to meet requirements of modern micro- and nano-electronic technologies [4].

Oblique deposition of atoms on a substrate is a well-known method for producing samples with well-defined uniaxial anisotropy [5,6]. Magnetic anisotropy arises as a consequence of a dipolar interaction of inhomogeneous column-like microstructure that develops in films because of self-shadowing effect [5–8]. Oblique deposition is used widely to produce multilayer films [9,10] and exchange bias systems [11] with accurate control of uniaxial anisotropy in individual layers. Note that most studies on magnetic anisotropy induced by oblique deposition have only been carried out for relatively large off-normal angles of incidence. However, we have recently reported that oblique deposition even for very small incident angles ($\sim 2^\circ$) strongly influences the magnetic characteristics of a thin permalloy film [12]. In the study, it was also shown that in the low-incidence angle deposition film the magnetic anisotropy that originates from oblique deposition is an important, but not necessarily dominant contribution in the resulting anisotropy.

The purpose of the present study is to explore the competitive relation between two close-in-value magnetic anisotropies induced by (i) oblique deposition with low-incidence angle and (ii) by magnetic field applied during sample growth. The central focus of our study is the effect of the anisotropies compensation obtained on local area of the thin permalloy film when their easy axes are mutually orthogonal. Our particular interest is related to the appearance of high-order magnetic anisotropies observed near the compensation point.

2. Experimental details

A sample was produced by thermal vacuum evaporation of $Ni_{82}Fe_{18}$ on a polished glass $10 \times 10 \times 0.5$ mm size substrate. The base pressure was lower than 10^{-6} mbar and the deposition rate was 1 nm/s. The distance between the vapor source and the substrate was 240 mm. The substrate was tilted so that the deposition beam struck the surface at a small angle with respect to the film normal. As illustrated in Fig. 1a, because of the conical trajectory of the deposited atoms, the incidence angle α changes gradually within the substrate from 7° to 9.2° along the x axis of the film

---

[*] Corresponding author.
E-mail address: platon.solovev@gmail.com (P.N. Solovev).

http://dx.doi.org/10.1016/j.physb.2015.10.036
0921-4526/© 2015 Elsevier B.V. All rights reserved.

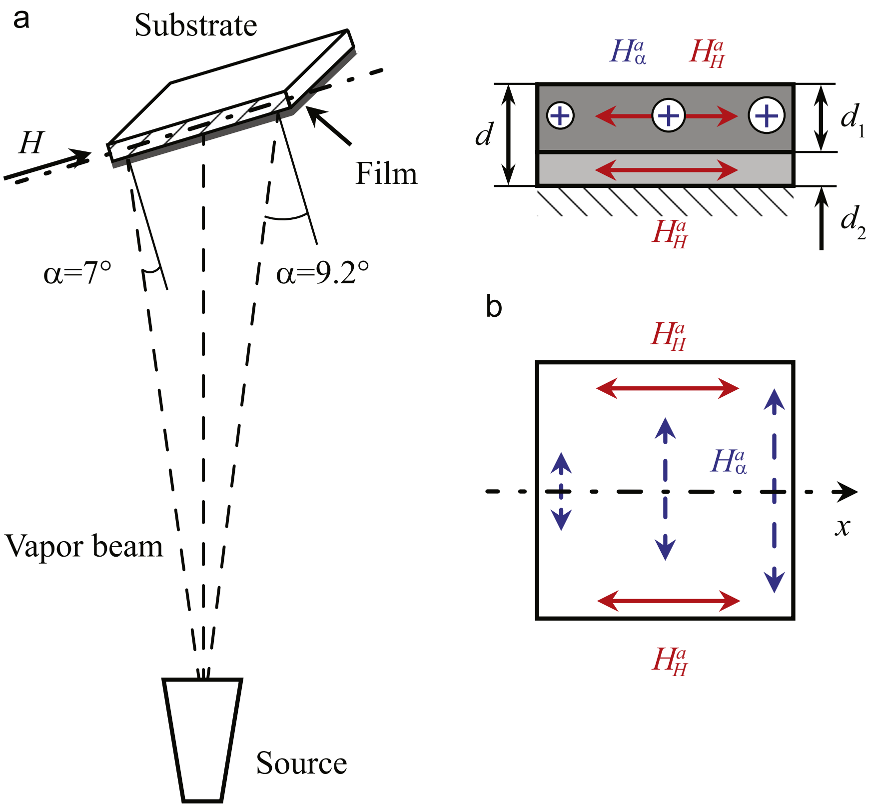

Fig. 1. (a) Sketch of the film deposition in the applied magnetic field *H*. (b) The bilayer model of the film with uniaxial anisotropies induced by magnetic field H^a_H and oblique deposition H^a_α.

depending almost linearly on the *x* coordinate. During the deposition, an orienting external magnetic field $H=200$ Oe was applied on the film plane. The direction of the magnetic field was set in such a way that the anisotropies induced by the field (H^a_H) and the oblique deposition (H^a_α) were mutually orthogonal. X-ray fluorescence analysis showed that the thickness of the sample *d* was 61 nm and its composition was $Ni_{83.7}Fe_{16.3}$.

Magnetic properties were analyzed by the scanning spectrometer of ferromagnetic resonance (FMR) [13]. The microstrip resonator fabricated on a dielectric substrate was used as a sensor in the spectrometer. The measuring hole was etched in the ground plane of the resonator near the antinode of high-frequency magnetic field. The hole diameter (~1 mm) determined the locality of measurements. Resonant absorption of microwaves by an investigated part of the magnetic film was registered by the modulation method through the change of the resonator quality factor during the sweeping of the static magnetic field. Because of the large filling factor of the microstrip resonator, the spectrometer had high sensitivity. The microwave pump frequency was 2.274 GHz for all measurements. Angular dependences of FMR field $H_R(\varphi_H)$ and linewidth $\Delta H(\varphi_H)$ were measured with 1 mm step along the *x* axis of the film, which was parallel to the external magnetic field.

For detailed analysis of the experimental data, we have developed a technique to extract information about high-order magnetic anisotropies from measured angular dependences of the resonance field. The analysis is based on the expression of the magnetic anisotropy energy in a form of a Fourier expansion versus in-plane azimuthal magnetization angle φ

$$F^a(\theta,\varphi)=\sum_n A_n(\theta)\cos n(\varphi-\varphi_n^a), \tag{1}$$

where θ means the angle between the magnetization and the normal to the film plane, $H^a_n=n^2A_n(\pi/2)/M_s$ and ϕ^a_n are effective field and direction of *n*-order in-plane magnetic anisotropy, and M_s is the saturation magnetization. Taking into account the Zeeman energy, the shape anisotropy of the film, and the uniaxial perpendicular anisotropy with constant $K_\perp$, the free energy density can be written as

$$F(\theta,\varphi)=-M_sH\cos(\varphi-\varphi_H)\sin\theta+2\pi M_s^2\cos^2\theta-K_\perp\cos^2\theta+F^a(\theta,\varphi). \tag{2}$$

In low-dimensional systems such as thin films, a shape anisotropy energy is usually the dominant term in the total magnetic anisotropy energy. The shape anisotropy is the main reason of in-plane orientation of the magnetization in the sample. The reorientation of the spontaneous magnetization from the film plane to the normal because of the surface anisotropy is possible only for ultrathin films with thicknesses of a few atomic layers [14]. Therefore, when the film is magnetized by the in-plane external magnetic field, the equilibrium angle θ equals $\pi/2$.

Using the Smith and Suhl formula [15,16], the ferromagnetic resonance equation and equilibrium condition can be written as follows:

$$\left[H_R\cos(\varphi_M-\varphi_H)+\frac{F^a_{\varphi\varphi}}{M_s}\right]\times\left[H_R\cos(\varphi_M-\varphi_H)+4\pi M_{eff}+\frac{F^a_{\theta\theta}}{M_s}\right]-\frac{F^{a2}_{\theta\varphi}}{M_s^2}=\left(\frac{\omega_0}{\gamma}\right)^2, \tag{3}$$

$$H_R\sin(\varphi_M-\varphi_H)+F^a_\varphi/M_s=0, \tag{4}$$

where $f_0=\omega_0/2\pi$ is the microwave pump frequency, γ is the gyromagnetic ratio and M_{eff} is the effective magnetization ($4\pi M_{eff}=4\pi M_s-2K_\perp/M_s$). The partial derivatives of $F^a_{\phi\phi}$, $F^a_{\theta\theta}$, $F^a_{\theta\phi}$, and F^a_ϕ have to be taken at the equilibrium position of the magnetization vector, that is, for angles $\theta=\pi/2$ and $\varphi=\varphi_M$, for which the total free energy density F has its minimum value.

The effective demagnetization field $4\pi M_{eff}$ plays an important role in the FMR measurements. For not very thin films, its value significantly exceeds magnetic anisotropy fields. For example, $4\pi M_{eff}\sim 10^4$ Oe, whereas $2K_1/M_s\sim 10^2$ Oe for monocrystalline iron films [17]. This can be used for the approximate solutions of Eqs. (3) and (4) by neglecting terms $F^a_{\theta\theta}$ and $F^a_{\theta\phi}$. It is necessary because, for the general case, the analytical expression $A_n(\theta)$ in F^a expansion is unknown. Then the FMR and equilibrium conditions are

$$\left[H_R\cos(\varphi_M-\varphi_H)-\sum_n H_n^a\cos n(\varphi_M-\varphi_n^a)\right]\times \left[H_R\cos(\varphi_M-\varphi_H)+4\pi M_{eff}\right]=\left(\frac{\omega_0}{\gamma}\right)^2, \tag{5}$$

$$H_R\sin(\varphi_M-\varphi_H)-\sum_n \frac{H_n^a}{n}\sin n(\varphi_M-\varphi_n^a)=0. \tag{6}$$

We have derived the following expression for the estimation of the absolute error ΔH_ε that originates from the approximation

$$\Delta H_\varepsilon\approx\left|(H_n^a)_{\max}\frac{(\omega_0/\gamma)^2}{(4\pi M_{eff})^2}\right|, \tag{7}$$

where $(H_n^a)_{\max}$ is a maximum measured anisotropy field. To determine the experimental parameters of the magnetic anisotropy H_n^a and ϕ_n^a, we implemented a numerical procedure that allows approximating the experimental angular dependence $H_R(\varphi_H)$ of theoretical curve calculated using nonlinear Eqs. (5) and (6). Note that the observed experimental error ΔH_ε was no more than 0.06 Oe.

3. Results and discussion

Fig. 2 shows the experimental results of the resonance field H_R and the FMR linewidth ΔH as a function of the sweeping field direction φ_H for the three points of the sample with coordinates $x=-2$ mm ($\alpha=7.6°$), 1 mm ($\alpha=8.3°$), and 4 mm ($\alpha=9.0°$) with respect to the film center. The solid lines on Fig. 2a are numerical fits to the experimental data according to Eqs. (5) and (6). The dependences $H_R(\varphi_H)$ demonstrate that the variation of the deposition angle leads to the significant change in the magnetic anisotropy value and direction. Moreover, for certain angles, the very character of the anisotropy is changed.

The results retrieved from angular dependences of the resonance field show that there is a significant contribution of high-order effective anisotropies to the resulting magnetic anisotropy. Fig. 3 displays the effective parameters of dominant contributions to the energy F^a, which were obtained for each measured point of the sample. The open and closed symbols represent the values of H_n^a and ϕ_n^a accordingly. The dependencies of the uniaxial anisotropy value $H_2^a(x)$ and direction $\phi_2^a(x)$ (Fig. 3) demonstrate the competition between the two mechanisms that form the resulting magnetic anisotropy. For small incidence angles ($x<1$ mm), the main source of the magnetic anisotropy is the magnetic field applied during deposition. Hence, the easy magnetization axis ($\phi_2^a\approx 1.5°$) lies nearly in the direction of the orienting external magnetic field. The increase of the deposition angle α leads to the growth of the anisotropy H_α^a induced by oblique deposition. Therefore, even as α grows, the uniaxial anisotropy field H_2^a at first significantly decreases and then increases almost to the same value. For the deposition angle of about 8.3° ($x=1$ mm), the anisotropy has a minimum value showing that the anisotropies induced by magnetic field H_H^a and by oblique deposition H_α^a almost compensate each other in this area of the sample. For greater angles ($x>1$ mm), oblique deposition becomes the dominant source of the anisotropy resulting in the dramatic rotation of ϕ_2^a at 80° toward the easy axis direction of obliquely induced anisotropy H_α^a.

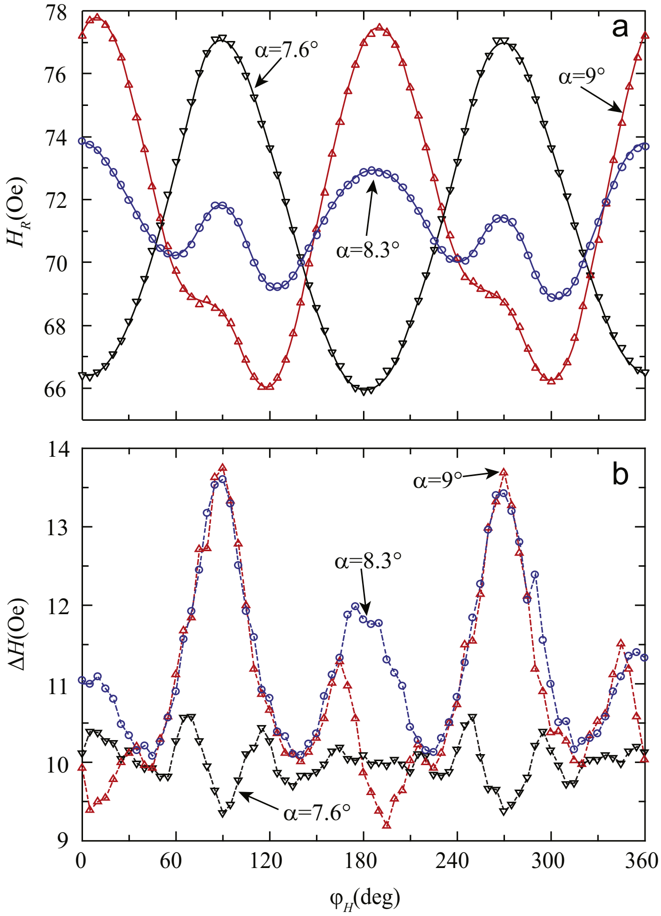

Fig. 2. Measured (markers) and theoretical (solid lines) dependences of the resonance field H_R (a) and the FMR linewidth ΔH (b) on the sweeping field direction φ_H obtained from local areas of the sample at points $x=-2$ mm ($\alpha=7.6°$), $x=1$ mm ($\alpha=8.3°$), and $x=4$ mm ($\alpha=9.0°$).

The revealed uniaxial anisotropy compensation effect is the result of a simple summation for mutually orthogonal anisotropies of different nature with close values. For example, similar compensation effect was observed in magnetostrictive films in which easy axes of stress-induced and field-induced uniaxial anisotropies were at right angles [18]. However, contrary to the earlier results, in addition to the uniaxial anisotropy, the effective anisotropies of fourfold and sixfold symmetry are clearly observed in the sample.

Fig. 3 shows parameters of the fourfold and sixfold effective anisotropies extracted from FMR angular dependences measured on local areas of the sample. The magnitude of the fourfold effective anisotropy H_4^a significantly increases with increasing of the deposition angle α, whereas the easy direction $\phi_4^a(x)$ changes slightly. At the compensation point ($x=1$ mm), the magnitude $H_4^a=1.16$ Oe is close to the value of the uniaxial anisotropy ($H_2^a=1.37$ Oe). For $x=2$ mm, the fourfold anisotropy field has a maximum 1.52 Oe. The magnitude of sixfold effective anisotropy H_6^a increases almost monotonically with α; however, it shows a local maximum at the compensation point. The value of the sixfold anisotropy field is below 0.5 Oe for the whole sample. The presence of the high-order contributions H_4^a and H_6^a in the resulting anisotropy can indicate that the film consists of exchange-coupled adjacent regions or phases with different magnetic parameters

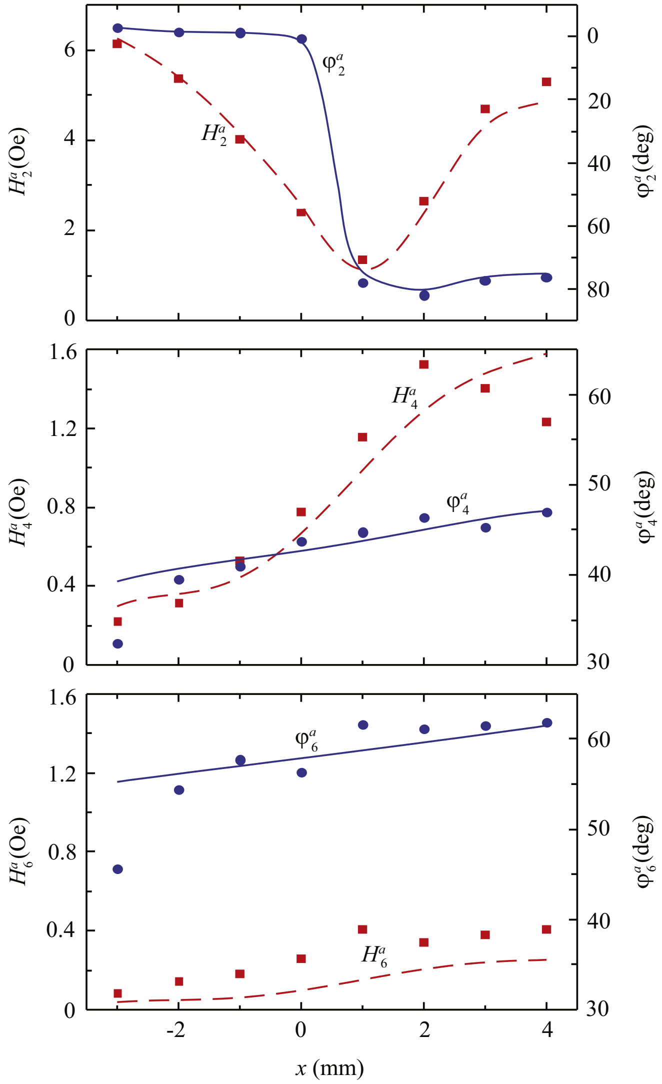

Fig. 3. The magnitudes (left axes) and directions (right axes) of the effective anisotropies of second, fourth, and sixth order as a function of the x coordinate. Markers and lines accordingly represent values retrieved from experimental and micromagnetic simulation FMR angular dependences.

[19,20]. Particularly, it was experimentally observed and theoretically confirmed that bilayer systems with orthogonally oriented uniaxial anisotropies in each layer display a fourfold effective magnetic anisotropy [21–23]. Similar models were also used to analytically explain the magnetization dynamics features in magnetically nonuniform thin films [24,25].

Off-normal deposition leads to a formation of a heterogeneous morphology in a microcrystalline structure of a film due to geometric shadowing mechanism. If the heterogeneity has an anisotropic character, then it will be a source of magnetic anisotropy because of the dipolar interaction. Studies [26,27] of films morphology show that porosity, roughness, and other heterogeneities of microcrystalline structure generally increase as the thickness of a film increases from substrate to top. Therefore, at a first approximation, an obliquely deposited film can be considered as a two-layer exchange-coupled magnetic structure characterized by certain averaged parameters (Fig. 1b). Within the framework of this hypothesis, we assume that the lower layer of the film with thickness d_1 is almost uniform. This means that the magnetic anisotropy attributed to oblique deposition is absent in the lower layer. However, the external magnetic field applied during deposition induces uniaxial anisotropy in it. On the other hand, the top layer of the film is characterized by the anisotropy induced by oblique deposition with averaged through the thickness effective parameters H^a_α and ϕ^a_α, and the field-induced anisotropy with effective parameters H^a_H and ϕ^a_H. We assume for simplicity that the magnetization saturation M_s, the exchange constant A, and the parameters H^a_H and ϕ^a_H have constant values for the whole film.

We have performed micromagnetic simulation of the two-layer film model to validate the proposed hypothesis using our micromagnetic modeling tool. The calculations of static properties are based on the free energy minimization for each applied magnetic field using Lagrange multiplier method [28]. The obtained ground state is then used for evaluation of magnetization oscillations normal modes by linearization of Landau–Lifshitz–Gilbert equation [29,30]. The calculations were performed under in-plane periodic boundary conditions for magnetostatic and exchange interactions [31].

Similar to the experiment, effective magnetic anisotropy fields and corresponding easy directions of magnetization have been retrieved from calculated resonance field angular dependences. Micromagnetic analysis allowed us to find optimal parameters of the theoretical model for which the calculated results fit to the experimental data: the thickness of the lower layer is $d_1 = 12.2$ nm ($d_1/d = 0.2$), the magnetization saturation is $M_s = 734$ G, the exchange constant is $A = 0.025 \times 10^6$ erg/cm, and the damping coefficient is 0.0062. The magnitude of the field-induced anisotropy $H^a_H = 14.4$ Oe and its easy direction $\phi^a_H = -2.07°$ are constant for the whole film. The optimal fit parameters of the anisotropy induced by oblique deposition, that is, the magnitude H^a_α and the easy axis direction ϕ^a_α, depend on the deposition angle (or corresponding coordinate x) (Fig. 4).

Lines on Fig. 3 demonstrate the parameters of the effective magnetic anisotropies obtained by the micromagnetic analysis of the two-layer film model, as a function of the x coordinate. A good agreement between theoretical and experimental results confirms the applicability of the two-layer model for explaining the existence of the high-order effective magnetic anisotropies in the thin film produced by oblique deposition in an applied magnetic field. However, this simple model does not explain the decrease of the effective fourfold anisotropy field for $x > 2$ mm ($\alpha > 8.5°$) observed in the experiment. In addition, the calculated values of the effective sixfold anisotropy is approximately two times smaller than the experimental ones.

Note that observed in the experiment broadening of the FMR line for points $x = 1$ mm and $x = 4$ mm (Fig. 2b) is an evidence to support the proposed hypothesis. It is shown in Ref. [24] that because of a nonuniform magnetization state in samples consisting of two soft exchange coupled magnetic layers with in-plane easy axes at right angles, the uniform high-frequency field can

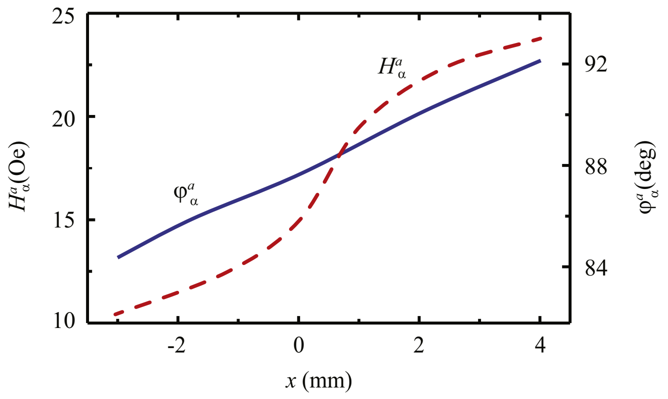

Fig. 4. The fit parameters of the obliquely induced magnetic anisotropy as a function of x coordinate.

excite a series of resonance FMR modes. We assume that superposition of the resonance peaks of these modes leads to the observed in Fig. 2b broadening of the FMR line.

4. Conclusion

In this research, we have studied the nature of the magnetic anisotropy developed in the thin permalloy film fabricated by the oblique deposition with the small incidence angles in the applied magnetic field oriented orthogonally to the deposition plane. The investigation was performed using local spectrometer of ferromagnetic resonance and micromagnetic simulation. We have observed the compensation of the uniaxial anisotropy. Moreover, we have experimentally discovered the formation of the fourfold and sixfold effective anisotropies. The revealed effects have been explained in the framework of the proposed hypothesis, in which the film was assumed to consist of two exchange-coupled layers with different magnetic anisotropy parameters. The generally good agreement between results of the micromagnetic simulation and measurements confirmed the hypothesis.

Acknowledgments

This study was supported by the Ministry of Education and Science of the Russian Federation, task no. 3.528.2014K.

References

[1] J. Lindner, M. Farle, Magnetic anisotropy of heterostructures, STMP 227 (2007) 45, http://dx.doi.org/10.1007/978-3-540-73462-8_2.

[2] A.N. Lagarkov, I.T. Iakubov, I.A. Ryzhikov, K.N. Rozanov, N.S. Perov, E.P. Elsukov, S.A. Maklakov, A.V. Osipov, M.V. Sedova, A.M. Getman, A.L. Ulyanov, Fe–N films: morphology, static and dynamic magnetic properties, Physica B 394 (2007) 159, http://dx.doi.org/10.1016/j.physb.2006.12.086.

[3] D. Sander, The magnetic anisotropy and spin reorientation of nanostructures and nanoscale films, J. Phys.: Condens. Matter 16 (2004) R603, http://dx.doi.org/10.1088/0953-8984/16/20/R01.

[4] J.P. Volkerts, Magnetic Thin Films: Properties, Performance and Applications, Nova Science Publishers, Incorporated (2011), p. 409.

[5] D.O. Smith, M.S. Cohen, G.P. Weiss, Oblique Incidence Anisotropy in Evaporated Permalloy Films, J. Appl. Phys. 31 (1960) 1755, http://dx.doi.org/10.1063/1.1735441.

[6] Matthew M. Hawkeye, Michael J. Brett, Glancing angle deposition: Fabrication, properties, and applications of micro- and nanostructured thin films, J. Vac. Sci. Technol. A 25 (2007) 1317, http://dx.doi.org/10.1116/1.2764082.

[7] C. Quiros, L. Peverini, J. Diaz, A. Alija, C. Blanco, M. Velez, O. Robach, E. Ziegler, J.M. Alameda, Asymmetric grazing incidence small angle X-ray scattering and anisotropic domain wall motion in obliquely grown nanocrystalline Co films, Nanotechnol 25 (2014) 335704, http://dx.doi.org/10.1088/0957-4484/25/33/335704.

[8] A. Keller, L. Peverini, J. Grenzer, G.J. Kovacs, A. Mucklich, S. Facsko, Polycrystalline Ni thin films on nanopatterned Si substrates: From highly conformal to nonconformal anisotropic growth, Phys. Rev. B 84 (2011) 035423, http://dx.doi.org/10.1103/PhysRevB.84.035423.

[9] L.M. Alvarez-Prado, S.M. Valvidares, J.I. Martin, J.M. Alameda, Competing magnetic anisotropies in exchange coupled bilayers with growth-induced orthogonal uniaxial axes, Phys. Rev. B 76 (2007) 214419, http://dx.doi.org/10.1103/PhysRevB.76.214419.

[10] Xiaoxi Zhong, Nguyen N. Phuoc, Ying Liu, C.K. Ong, Employment of Co underlayer and oblique deposition to obtain high resonance frequency and excellent thermal stability in FeCo thin films, J. Magn. Magn. Mater. 365 (2014) 8, http://dx.doi.org/10.1016/j.jmmm.2014.04.046.

[11] R.L. Rodriguez-Suarez, L.H. Vilela-Leao, T. Bueno, J.B.S. Mendes, P. Landeros, S. M. Rezende, A. Azevedo, Tunable misalignment of ferromagnetic and antiferromagnetic easy axes in exchange biased bilayers, Appl. Phys. Lett. 100 (2012) 242406, http://dx.doi.org/10.1063/1.4729040.

[12] B.A. Belyaev, A.V. Izotov, P.N. Solovev, The effect of oblique deposition with small incidence on magnetic properties of thin magnetic films, Solid State Phenom. 215 (2014) 223, http://dx.doi.org/10.4028/www.scientific.net/SSP.215.223.

[13] B.A. Belyaev, A.V. Izotov, A.A. Leksikov, Magnetic imaging in thin magnetic films by local spectrometer of ferromagnetic resonance, IEEE Sens. 5 (2005) 260, http://dx.doi.org/10.1109/JSEN.2004.842293.

[14] M.T. Johnson, P.J.H. Bloemen, F.J.A. Den Broeder, J.J. De Vries, Magnetic anisotropy in metallic multilayers, Rep. Prog. Phys. 59 (11) (1996) 1409, http://dx.doi.org/10.1088/0034-4885/59/11/002.

[15] J. Smit, H. Beljers, Ferromagnetic resonance absorption in $BaFe_{12}O_{19}$, a highly anisotropic crystal, Philips Res. Rep. 10 (1955) 113.

[16] H. Suhl, Ferromagnetic resonance in nickel ferrite between one and two kilomegacycles, Phys. Rev. 97 (2) (1955) 555, http://dx.doi.org/10.1103/PhysRev.97.555.2.

[17] G.A. Prinz, Magnetic metal films on semiconductor, Ultrathin Magnetic Structures II, Springer. P., Berlin (1994), p. 1–44, http://dx.doi.org/10.1007/978-3-540-27166-6.

[18] B.A. Belyaev, A.V. Izotov, Ferromagnetic resonance study of the effect of elastic stresses on the anisotropy of magnetic films, Phys. Solid State 49 (2007) 1731, http://dx.doi.org/10.1134/S106378340709020X.

[19] E.J. Torok, H.N. Oredson, A.L. Olson, Local regions with biaxial anisotropy in thin polycrystalline ferromagnetic films with uniaxial anisotropy, J. Appl. Phys. 35 (1964) 3469, http://dx.doi.org/10.1063/1.1713253.

[20] A. Yelon, HighOrder anisotropies in uniaxial magnetic films, J. Appl. Phys. 38 (1967) 325, http://dx.doi.org/10.1063/1.1708975.

[21] E. Goto, N. Hayashi, T. Miyashita, K. Nakagawa, Magnetization and switching characteristics of composite thin magnetic films, J. Appl. Phys. 36 (1965) 2951, http://dx.doi.org/10.1063/1.1714613.

[22] B. Valcu, E. Girt, A. Dobin, Second order anisotropy in exchange spring systems, IEEE Trans. Magn. 44 (2008) 3554, http://dx.doi.org/10.1109/TMAG.2008.2001790.

[23] S.M. Valvidares, L.M. Alvarez-Prado, J.I. Martin, J.M. Alameda, Inverted hysteresis loops in magnetically coupled bilayers with uniaxial competing anisotropies: theory and experiments, Phys. Rev. B 64 (2001) 134423, http://dx.doi.org/10.1103/PhysRevB.64.134423.

[24] V. Dubuget, A. Thiaville, F. Duverger, S. Dubourg, O. Acher, A. Adenot-Engelvin, Magnetization dynamics of soft films with thickness-dependent anisotropy, Phys. Rev. B 80 (2009) 134412, http://dx.doi.org/10.1103/PhysRevB.80.134412.

[25] V. Dubuget, S. Dubourg, P. Thibaudeau, F. Duverger, Magnetic anisotropy dispersion with exchange energy in soft ferromagnetic thin films, IEEE Trans. Magn. 46 (2010) 1139, http://dx.doi.org/10.1109/TMAG.2010.2040187.

[26] K. Kaminska, A. Amassian, L. Martinu, K. Robbie, Growth of vacuum evaporated ultraporous silicon studied with spectroscopic ellipsometry and scanning electron microscopy, J. Appl. Phys. 97 (2005) 013511, http://dx.doi.org/10.1063/1.1823029.

[27] A. Amassian, K. Kaminska, M. Suzuki, L. Martinu, K. Robbie, Onset of shadowing-dominated growth in glancing angle deposition, Appl. Phys. Lett. 91 (2007) 173114, http://dx.doi.org/10.1063/1.2794420.

[28] B.A. Belyaev, A.V. Izotov, Micromagnetic calculation of the equilibrium distribution of magnetic moments in thin films, Phys. Solid State 52 (2010) 1664, http://dx.doi.org/10.1134/S1063783410080160.

[29] A.V. Izotov, B.A. Belyaev, A method for computing the microwave absorption spectrum in a discrete model of a ferromagnetic, Russ. Phys. J. 53 (2011) 900, http://dx.doi.org/10.1007/s11182-011-9508-4.

[30] B.A. Belyaev, A.V. Izotov, Micromagnetic calculation of magnetostatic oscillation modes of an orthogonally magnetized disk of yttrium iron garnet, Phys. Solid State 55 (2013) 2491, http://dx.doi.org/10.1134/S1063783413120068.

[31] K.M. Lebecki, M.J. Donahue, M.W. Gutowski, Periodic boundary conditions for demagnetization interactions in micromagnetic simulations, J. Phys. D: Appl. Phys. 41 (2008) 175005, http://dx.doi.org/10.1088/0022-3727/41/17/175005.